PERGAMON

Journal of the Mechanics and Physics of Solids
49 (2001) 979–993

JOURNAL OF THE
MECHANICS AND
PHYSICS OF SOLIDS

www.elsevier.com/locate/jmps

Fracture in mechanism-based strain gradient plasticity

H. Jiang[a], Y. Huang[a,b,*], Z. Zhuang[a], K.C. Hwang[a]

[a] *Failure Mechanics Key Laboratory, Department of Engineering Mechanics, Tsinghua University, Beijing 100084, China*

[b] *Department of Mechanical and Industrial Engineering, University of Illinois, Urbana, IL 61801, USA*

Received 12 July 2000; received in revised form 21 August 2000; accepted 17 October 2000

Abstract

In a remarkable series of experiments, Elssner, Korn and Ruehle (Scripta Metall. Mater. 31 (1994) 1037) observed cleavage fracture in ductile materials, a phenomenon that cannot be explained by classical plasticity theories. In this paper we present a study of fracture by the theory of mechanism-based strain gradient (MSG) plasticity (Gao et al., J. Mech. Phys. Solids 47 (1999b) 1239); Huang et al., J. Mech. Phys. Solids 48 (2000a) 99). It is established that, at a distance much larger than the dislocation spacing such that continuum plasticity is applicable, the stress level in MSG plasticity is significantly higher than that in classical plasticity near the crack tip. The numerical results also show that the crack tip stress singularity in MSG plasticity is higher than that in the HRR field, and it exceeds or equals to the square-root singularity. This study provides a means to explain the observed cleavage fracture in ductile material.

Keywords: A. Fracture; Mechanism-based strain gradient plasticity

1. Introduction

1.1. Macroscopic and atomistic fracture

In a remarkable series of experiments, Elssner et al.'s (1994) measured both the macroscopic fracture toughness and atomic work of separation of an interface between a single crystal of niobium and a sapphire single crystal. The macroscopic work of fracture was measured using a four-point bend specimen designed for the determination of

* Corresponding author. Tel.: +1-217-265-5072; fax: +1-217-244-6534.
E-mail address: huang9@uiuc.edu (Y. Huang).

0022-5096/01/$ - see front matter
PII: S0022-5096(00)00070-3

interfacial toughness, while the atomic value was inferred from the equilibrium shapes of microscopic pores on the interface. The macroscopic work of fracture was found to be 2–3 orders of magnitude higher than the atomic work of separation. This large difference between the macroscopic work of fracture and its counterpart at the atomic level was attributed to plastic dissipation in niobium, i.e., there must be significant plastic deformation associated with dislocation activities in niobium. Therefore, the crack tip should be blunted by dislocations in niobium. According to models based on the classical theories of plasticity, the maximum stress level that can be achieved near a crack tip is no more than 4–5 times the tensile yield stress of metals (Hutchinson, 1997). However, Elssner et al.'s (1994) observed that the interface between two materials remained atomistically sharp, i.e., the crack tip was not blunted even though niobium had a large number of dislocations. Moreover, the stress level needed to produce atomic decohesion of a lattice or a strong interface is typically 3% of the Young's modulus, or 10 times the tensile yield stress, which is more than twice the maximum stress level (4–5 times yield stress) predicted by classical plasticity theories.

Classical plasticity theories clearly fall short of triggering the atomic decohesion observed in the Elssner et al.'s (1994) experiments. As Hutchinson (1997) pointed out, attempts to link macroscopic cracking to atomistic fracture are frustrated by the inability of classical plasticity theories to model stress–strain behavior adequately at the small scales involved in crack tip deformation.

There are significant efforts to develop continuum plasticity models which predict much higher stress level near the crack tip than classical plasticity theories do in order to explain the atomistically sharp crack tip in ductile niobium observed in the Elssner et al.'s (1994) experiments. Suo et al. (1993) proposed a model (referred as the SSV model in the following) that embeds an elastic strip surrounding the crack tip. The height of the strip is very small, on the order of dislocation spacing, such that dislocation activities within the strip cannot be homogenized and represented by continuum plasticity theories. Therefore, the strip is modeled as a linear elastic medium such that the elastic strip around the crack tip is surrounded by a plastic zone. The existence of such an elastic strip indeed increases the stress level near the crack tip. Beltz et al. (1996) extended the SSV model (Suo et al., 1993) to provide a self-consistent estimate of the strip height based on dislocation analysis, and confirmed that the strip height is indeed on the order of dislocation spacing. Wei and Hutchinson (1999) combined the SSV model with the embedded cohesion surface approach (Needleman, 1987; Tvergaard and Hutchinson, 1992, 1993; Xu and Needleman, 1994; Camacho and Ortiz, 1996) to investigate the stress level around a crack tip.

An alternative approach that has the potential to bridge the gap between the atomistic fracture and macroscopic cracking comes from strain gradient plasticity theories. Strain gradient plasticity theories have been developed primarily for another important class of phenomena at small scales, namely the size effect. For example, micro-indentation experiments have repeatedly shown that the hardness of metallic materials is doubled or even tripled as the depth of indentation decreases to microns or submicrons (Nix, 1989, 1997; De Guzman et al., 1993; Stelmashenko et al., 1993; Atkinson, 1995; Ma and Clarke, 1995; Poole et al., 1996; McElhaney et al., 1998). Significant increase in strength has also been observed in micro-torsion of thin copper wires

(Fleck et al., 1994), micro-bend of thin nickel foils (Stolken and Evans, 1998), and in particle-reinforced composites (Lloyd, 1994; Nan and Clarke, 1996). These experiments have all shown that materials display strong size effect, "the smaller the harder". Classical plasticity theories cannot explain the observed size effect at the small scales because their constitutive models possess no internal material lengths.

Based on the notion of geometrically necessary dislocations in dislocation mechanics (Ashby, 1970), Fleck, Hutchinson and co-workers (Fleck and Hutchinson, 1993, 1997; Fleck et al., 1994; Shu and Fleck, 1999) have developed a strain gradient plasticity theory, intended for applications to materials and structures whose dimension controlling plastic deformation falls roughly within a range from a tenth of a micron to ten microns. Strain gradients are introduced into the constitutive model, and the internal material length scaling the strain gradients has been determined to be on the order of microns. There also exist several alternative theories of strain gradient plasticity that are also based on the notion of geometrically necessary dislocations (e.g., Arsenlis and Parks, 1999; Gao et al., 1999b; Acharya and Bassani, 2000; Gurtin, 2000; Huang et al., 2000a), while all these theories have some success in modeling the microscale experiments, only two have been applied to fracture analysis, as discussed in the following.

1.2. Fracture in strain gradient plasticity

The theories of strain gradient plasticity have been applied to fracture analyses in anticipation that they may provide a link between macroscopic cracking and atomistic fracture. This is because the stress level may increase significantly due to large strain gradients near the crack tip. The analyses are essentially limited to the couple-stress theory of strain gradient plasticity (Fleck and Hutchinson, 1993; Fleck et al., 1994) and the general phenomenological theory of strain gradient plasticity (Fleck and Hutchinson, 1997).

For the couple-stress theory of strain gradient plasticity, Huang et al. (1995, 1997b) and Xia and Hutchinson (1996) obtained analytically the plane-strain modes I, II and mixed mode asymptotic crack tip fields, while Chen et al. (1998) used the numerical shooting method to obtain the plane-stress asymptotic crack tip fields. The finite element method was also used to study the strain gradient effects near the crack tip (Xia and Hutchinson, 1996; Huang et al., 1997a, 1999a). It is established that the stress level estimated by the couple-stress theory of strain gradient plasticity near a mode-I crack tip is essentially the same as that in classical plasticity, i.e., no significant increase in the stress level around the mode-I crack tip is observed. This is because the couple-stress theory of strain gradient plasticity accounts for the rotation gradient of deformation only, and has not accounted for the important effect of stretch gradient near the crack tip.

In order to include the effect of stretch gradient, Wei and Hutchinson (1997) and Chen et al. (1999) used the Fleck and Hutchinson's (1997) general phenomenological strain gradient plasticity theory to investigate the crack tip field. The numerical results have shown that stretch gradients indeed elevate the stress level around a steadily propagating crack tip (Wei and Hutchinson, 1997). However, for a stationary crack tip, both the numerical shooting method and the finite element analysis predict a compressive

stress traction ahead of a mode-I crack tip (Chen et al., 1999), which is physically unacceptable. In order to solve this puzzle, Shi et al. (2000b) used the Wiener-Hopf technique of analytic continuation to obtain the full-field solution for the Fleck and Hutchinson (1997) general theory of strain gradient plasticity with the plastic work hardening exponent $N = 1$. The analytic full-field solution clearly demonstrated that the normal stress traction switches from tensile to compressive as the crack tip is approached. It is therefore concluded that the asymptotic crack tip field in the Fleck and Hutchinson (1997) general phenomenological theory of strain gradient plasticity has no domain of physical validity.

The theory of mechanism-based strain gradient (MSG) plasticity was established from the Taylor dislocation model via a multiscale, hierarchical framework in order to link mesoscale strain gradient plasticity to microscale dislocation mechanics. Gao et al. (1999a) and Huang et al. (2000b) have shown that the MSG plasticity theory agrees very well with micro-indentation (McElhaney et al., 1998), micro-bend (Stolken and Evans, 1998) and micro-torsion experiments (Fleck et al., 1994). Shi et al. (2000a) used MSG plasticity theory to investigate the asymptotic crack tip field, and established that, unlike the HRR field (Hutchinson, 1968; Rice and Rosengren, 1968) in classical plasticity, the asymptotic crack tip field in MSG plasticity is not separable. Therefore, the stress level around a crack tip in MSG plasticity can only be obtained by the finite element method or other numerical methods.

The purpose of this paper is to study fracture in MSG plasticity via the finite element method. It focuses on the increase of stress level around the crack tip due to strain gradient effects associated with the geometrically necessary dislocations in order to explain the observed cleavage fracture in ductile materials (Elssner et al., 1994). The results show the transition from the remotely imposed elastic K field through a plastic zone to the crack tip field in MSG plasticity.

2. Mechanism-based strain gradient (MSG) plasticity

The theory of mechanism-based strain gradient plasticity (Gao et al., 1999b; Huang et al., 1999b, 2000a) is summarized in this section.

2.1. Generalized stresses and strains

In a Cartesian reference frame x_i, the strain tensor ε_{ij} and strain gradient tensor η_{ijk} are related to the displacement u_i by

$$\varepsilon_{ij} = \tfrac{1}{2}(u_{i,j} + u_{j,i}) \tag{1}$$

and

$$\eta_{ijk} = u_{k,ij}, \tag{2}$$

which have the symmetry $\varepsilon_{ij} = \varepsilon_{ji}$ and $\eta_{ijk} = \eta_{jik}$. The strain gradient tensor can also be expressed directly in terms of the strain tensor, i.e.,

$$\eta_{ijk} = \varepsilon_{ik,j} + \varepsilon_{jk,i} - \varepsilon_{ij,k}. \tag{3}$$

The deviatoric strain and deviatoric strain gradient are defined as

$$\varepsilon'_{ij} = \varepsilon_{ij} - \tfrac{1}{3}\varepsilon_{kk}\delta_{ij}, \quad \eta'_{ijk} = \eta_{ijk} - \tfrac{1}{4}(\delta_{ik}\eta_{jpp} + \delta_{jk}\eta_{ipp}). \tag{4}$$

The virtual work per unit volume of the solid due to a variation of displacement δu_i is

$$\delta w = \sigma_{ij}\delta\varepsilon_{ij} + \tau_{ijk}\delta\eta_{ijk}, \tag{5}$$

where the symmetric Cauchy stress σ_{ij} is the work conjugate of the variation of strain $\delta\varepsilon_{ij}$, and the symmetric higher-order stress τ_{ijk} is the work conjugate of the variation of strain gradient $\delta\eta_{ijk}$.

2.2. Principle of virtual work: equilibrium equations and boundary conditions

The principle of virtual work gives (Fleck and Hutchinson, 1997)

$$\int_v (\sigma_{ij}\delta\varepsilon_{ij} + \tau_{ijk}\delta\eta_{ijk})\,\mathrm{d}v = \int_v f_k\delta u_k\,\mathrm{d}v + \int_a \left(t_k\delta u_k + r_k\frac{\partial\delta u_k}{\partial n}\right)\mathrm{d}a + \int_c p_k\delta u_k|\mathrm{d}x|, \tag{6}$$

where f_k is the body force per unit volume, t_k and r_k are the stress traction and double stress traction on the surface, n is the normal of the surface, and p_k is the line force (per unit length) on the edge c intercepted by two smooth surfaces.

The equilibrium equations can be obtained from the principle of virtual work,

$$\sigma_{ik,i} - \tau_{ijk,ij} + f_k = 0. \tag{7}$$

The stress tractions t_k and double stress tractions r_k on the surface of the body are

$$t_k = n_i(\sigma_{ik} - \tau_{ijk,j}) - D_j(n_i\tau_{ijk}) + n_in_j\tau_{ijk}(D_qn_q), \tag{8}$$

$$r_k = n_in_j\tau_{ijk}, \tag{9}$$

where n_i is the unit normal to the surface and D_j is the surface-gradient operator given by

$$D_j = (\delta_{jk} - n_jn_k)\frac{\partial}{\partial x_k}. \tag{10}$$

On the surface of the body, the gradient $\partial/\partial x_j$ can be resolved into the above surface gradient D_j and a normal gradient n_jD, i.e.,

$$\frac{\partial}{\partial x_j} = D_j + n_jD, \tag{11}$$

where

$$D = n_k\frac{\partial}{\partial x_k}. \tag{12}$$

2.3. Constitutive equations in MSG plasticity

The deformation theory of MSG plasticity (Gao et al., 1999b; Huang et al., 2000a) is used in the present study since the deformation around a stationary crack tip field is nearly proportional. The uniaxial stress–strain relation can be written as

$$\sigma = \sigma_{\text{ref}} f(\varepsilon), \tag{13}$$

where σ_{ref} is a reference stress in uniaxial tension and f is a function of strain. For most ductile materials, the function f can be written as a power law relation

$$f(\varepsilon) = \varepsilon^N, \tag{14}$$

where N is the plastic work hardening exponent ($0 \leq N < 1$).

Plastic yielding occurs when the effective stress σ_{e} reaches the flow stress σ,

$$\sigma_{\text{e}} = \sigma, \tag{15}$$

where the effective stress $\sigma_{\text{e}} = (\frac{3}{2}\sigma'_{ij}\sigma'_{ij})^{1/2}$ is defined in terms of the deviatoric stress σ'_{ij}, and the flow stress in the mechanism-based strain gradient (MSG) plasticity theory (Gao et al., 1999b; Huang et al., 2000a) is obtained from Taylor's dislocation model as

$$\sigma = \sigma_{\text{ref}} \sqrt{f^2(\varepsilon) + l\eta}. \tag{16}$$

Here ε and η are the effective strain and effective strain gradient, respectively,

$$\varepsilon = \sqrt{\tfrac{2}{3}\varepsilon'_{ij}\varepsilon'_{ij}}, \quad \eta = \tfrac{1}{2}\sqrt{\eta'_{ijk}\eta'_{ijk}}, \tag{17}$$

and the characteristic material length l in (16) associated with strain gradient plasticity is given in terms of shear modulus μ and Burgers vector b by (Huang et al., 1999b)

$$l = 18\alpha^2 \left(\frac{\mu}{\sigma_{\text{ref}}}\right)^2 b, \tag{18}$$

where α is an empirical material constant in Taylor's dislocation model for plastic work hardening of ductile materials, and is between 0.2 and 0.5 (e.g. Nix and Gibeling, 1985). For metallic materials, the internal material length is indeed on the order of microns, consistent with the estimate by Fleck and Hutchinson (1997).

The constitutive equations in the deformation theory of MSG plasticity are

$$\sigma_{ij} = K\varepsilon_{kk}\delta_{ij} + \frac{2\sigma}{3\varepsilon}\varepsilon'_{ij}, \tag{19}$$

$$\tau_{ijk} = l_\varepsilon^2 \left[\frac{1}{6}K\eta^{\text{H}}_{ijk} + \frac{\sigma}{\varepsilon}(\Lambda_{ijk} - \Pi_{ijk}) + \frac{\sigma^2_{\text{ref}} f(\varepsilon) f'(\varepsilon)}{\sigma}\Pi_{ijk}\right], \tag{20}$$

where K is the elastic bulk modulus, the flow stress σ is given in (16), η^{H}_{ijk} is the volumetric part of strain gradient tensor,

$$\eta^{\text{H}}_{ijk} = \tfrac{1}{4}(\delta_{ik}\eta_{jpp} + \delta_{jk}\eta_{ipp}), \tag{21}$$

and Λ_{ijk} and Π_{ijk} are given by

$$\Lambda_{ijk} = \tfrac{1}{72}[2\eta'_{ijk} + \eta'_{kij} + \eta'_{kji} + \tfrac{1}{2}\delta_{ij}\eta_{kpp} + \tfrac{1}{3}\eta^{\mathrm{H}}_{ijk}], \tag{22}$$

$$\Pi_{ijk} = \frac{1}{54\varepsilon^2}\left[\varepsilon'_{mn}(\varepsilon'_{ik}\eta'_{jmn} + \varepsilon'_{jk}\eta'_{imn}) + \frac{1}{4}\eta_{qpp}(\varepsilon'_{ik}\varepsilon'_{jq} + \varepsilon'_{jk}\varepsilon'_{iq})\right]. \tag{23}$$

The length l_ε in (20) is the mesoscale cell size and is given by

$$l_\varepsilon = 10\frac{\mu}{\sigma_{\mathrm{Y}}}b, \tag{24}$$

where σ_{Y} is the yield stress in uniaxial tension.

It should be pointed out that, even though the material length in (18) depends on the reference stress σ_{ref}, the theory of MSG plasticity is independent of the choice of σ_{ref}. This is evident from the expression of flow stress in (16), where $\sigma^2_{\mathrm{ref}} f^2(\varepsilon)$ represents the uniaxial stress–strain relation, and the gradient term $\sigma^2_{\mathrm{ref}} l\eta$ becomes $18\alpha^2\mu^2 b\eta$, and both are independent of σ_{ref}.

3. Numerical analysis of fracture in MSG plasticity

The finite element method for MSG plasticity is based on the principle of virtual work in (6). Several finite elements have been developed for strain gradient theories that incorporate the effect of both stretch and rotation gradients of deformation. Begley and Hutchinson (1998) generalized Xia and Hutchinson's (1996) C_1 element in the study of micro-indentation hardness experiments. Shu et al. (1999) extended Xia and Hutchinson (1996) and Shu and Fleck's (1998) hybrid element to account for the effect of stretch gradients. Wei and Hutchinson (1997) developed a higher-order element to investigate steady-state crack propagation in strain gradient plasticity. Huang et al. (2000b) used these elements to study micro-indentation experiments, and found the hardness predicted by MSG plasticity agrees very well with experimental data of McElhaney et al. (1998). They also showed that the numerical results from these elements agree well with all the existing analytic solutions in strain gradient plasticity.

We use these finite elements to study the full-field solution of mode-I fracture in MSG plasticity. We have taken a circular domain of radius $10^3 l$ centered at the crack tip in our plane-strain finite element analysis, where l is the internal material length in MSG plasticity given in (18). Very fine mesh is used near the crack tip, around which the size of the smallest element is less than $10^{-3} l$. Efforts are made to ensure elements having aspect ratio close to 1. Mesh refinement and comparison of different elements have ensured that the numerical results are accurate.

The crack faces remain traction-free. The classical mode-I elastic K field is imposed on the outer boundary of the finite element domain (of radius $10^3 l$). The elastic stress intensity factor, K_I, of the remotely applied field increases monotonically such that there is no unloading. In order to better characterize plastic yielding, we have used the following elastic–plastic stress–strain relation in uniaxial tension to replace

(13) and (14):

$$\sigma = E\varepsilon, \quad \varepsilon < \frac{\sigma_Y}{E},$$

$$= \sigma_{ref}\varepsilon^N \quad \varepsilon \geq \frac{\sigma_Y}{E}, \tag{25}$$

where E is the elastic modulus, σ_Y the yield stress in uniaxial tension, N is the plastic work hardening exponent ($0 \leq N < 1$), and the reference stress σ_{ref} is given by $\sigma_{ref} = \sigma_Y(E/\sigma_Y)^N$.

In the following, stresses σ_{ij} are normalized by the yield stress σ_Y in uniaxial tension, while the distance r to the crack tip is normalized by the internal material length l in MSG plasticity. The normalized, remotely applied stress intensity factor is $K_I/\sigma_Y l^{1/2}$. The stress distribution then depends on the following nondimensional parameters: the plastic work hardening exponent N; the ratio of yield stress to elastic modulus, σ_Y/E; the Poisson's ratio v; and nondimensional stress intensity factor $K_I/\sigma_Y l^{1/2}$. It should be pointed out that the internal material length l has been used to normalize r and K_I, and does not appear explicitly in the nondimensional stress distributions. Accordingly, the normalized stress distributions do not depend on the Taylor coefficient α in (18). Unless otherwise specified, the numerical results presented in this paper are for the following set of nondimensional material properties:

$$N = 0.2, \quad \frac{\sigma_Y}{E} = 0.2\%, \quad v = 0.3. \tag{26}$$

Fig. 1 shows that normalized effective stress, σ_e/σ_Y, versus the nondimensional distance to the crack tip, r/l, ahead of the crack tip (at polar angle $\theta = 1.014^\circ$) predicted by MSG plasticity, where $\sigma_e = (\frac{3}{2}\sigma'_{ij}\sigma'_{ij})^{1/2}$ is the effective stress. The remotely applied stress intensity factor is $K_I/\sigma_Y l^{1/2} = 20$, while the nondimensional material properties are given in (26). The plastic zone size is a bit more than $10l$, as seen from the interception of MSG plasticity curve with the horizontal line of $\sigma_e/\sigma_Y = 1$ (representing plastic yielding). The corresponding stress distribution in classical plasticity (without strain gradient effects) is also shown in Fig. 1. It is observed that, outside the plastic zone (as determined by $\sigma_e/\sigma_Y \leq 1$), both MSG and classical plasticity theories give the same straight line of slope $-1/2$, corresponding to the elastic K_I field. The predictions of MSG and classical plasticity theories are also the same within the plastic zone at a distance larger than $0.3l$ to the crack tip. For a typical estimate of $l = 4$ μm for copper (Fleck et al., 1994; Gao et al., 1999a), the above result indicates that the strain gradient effects are significant within a zone of approximately 1 μm in copper. This agrees with the Xia and Hutchinson's (1996) estimate of the size of dominance zone for the asymptotic crack tip field in strain gradient plasticity. It is not unreasonable that the local dislocation density reaches $10^{14}/m^2$ near a crack tip in metallic materials, which gives an average dislocation spacing of 0.1 μm. Therefore, this zone of 1 μm size is much larger than the average dislocation spacing so that continuum plasticity is still applicable. Once the distance to the crack tip is less than $0.3l$, the effective stress predicted by MSG plasticity increases much quicker than its counterpart in classical plasticity. At a distance of $0.1l$ to the crack tip, which is approximately 0.4 μm for copper and is within the intended range of applications of MSG plasticity

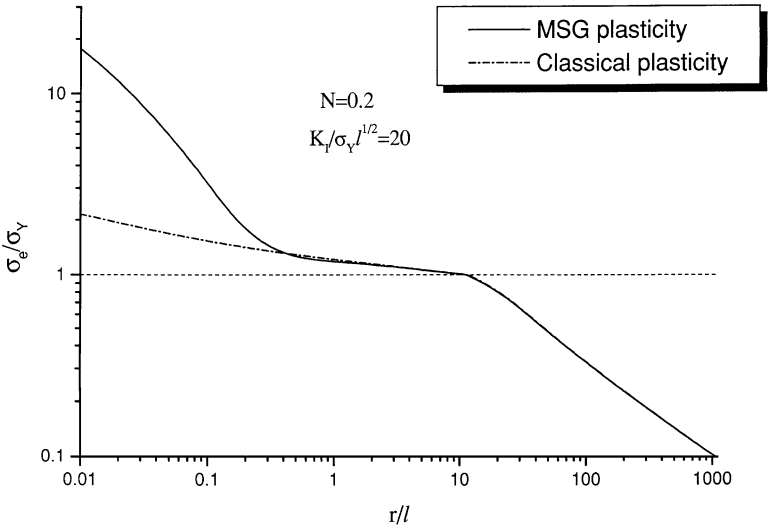

Fig. 1. The effective stress σ_e normalized by the uniaxial yield stress σ_Y versus the normalized distance to the crack tip, r/l, ahead of the crack tip (polar angle $\theta = 1.014^\circ$), where l is the internal material length in stain gradient plasticity; the plastic work hardening exponent $N = 0.2$, Poisson's ratio $v = 0.3$, the ratio of yield stress to elastic modulus $\sigma_Y/E = 0.2\%$, and the remotely applied elastic stress intensity factor $K_I/\sigma_Y l^{1/2} = 20$, the results are presented for both theories of MSG plasticity and classical plasticity.

(Gao et al., 1999b; Huang et al., 2000a), the effective stress given by MSG plasticity is more than twice that in classical plasticity. Moreover, for small distance to the crack tip (e.g., $r/l \leq 0.3$), classical plasticity gives a straight line in Fig. 1, and the slope of the straight line is $-N/(N+1)$, corresponding to the HRR field (Hutchinson, 1968; Rice and Rosengren, 1968) in classical plasticity. For $r/l \leq 0.3$, MSG plasticity gives a curve in Fig. 1, and the absolute value of the slope at each point on the curve not only is much larger than that for the HRR field ($|slope| = N/(N+1)$, but also exceeds or equals to that for elastic K_I field ($|slope| = \frac{1}{2}$). This indicates that stresses around a crack tip in MSG plasticity are more singular than the HRR field, and the order of stress singularity exceeds or equals to the square-root singularity.

Fig. 2 shows the normalized stresses, σ_{rr}/σ_Y and $\sigma_{\theta\theta}/\sigma_Y$, versus the nondimensional distance to the crack tip, r/l, ahead of the crack tip (polar angle $\theta = 1.014^\circ$) for both MSG plasticity and classical plasticity at the applied stress intensity factor $K_I/\sigma_Y l^{1/2} = 20$. The transition is clearly observed from the remote elastic K_I field (the straight line with slope $-1/2$ for large r) to the near-tip HRR field (the straight line with slope $-N/(N+1)$ for small r) in classical plasticity. The stress levels around the crack tip predicted by MSG plasticity and classical plasticity are different only within a distance of $0.3l$ to the crack tip, and the former is once again larger than the latter. Therefore, the strain gradient effects indeed elevate the stress level around the crack tip in MSG plasticity. It should be pointed out that the stress $\sigma_{\theta\theta}$ ahead of the crack tip is not the same as the stress traction t_θ defined in (8), and the difference results from the higher-order stresses. However, the contribution from the higher-order stresses is very

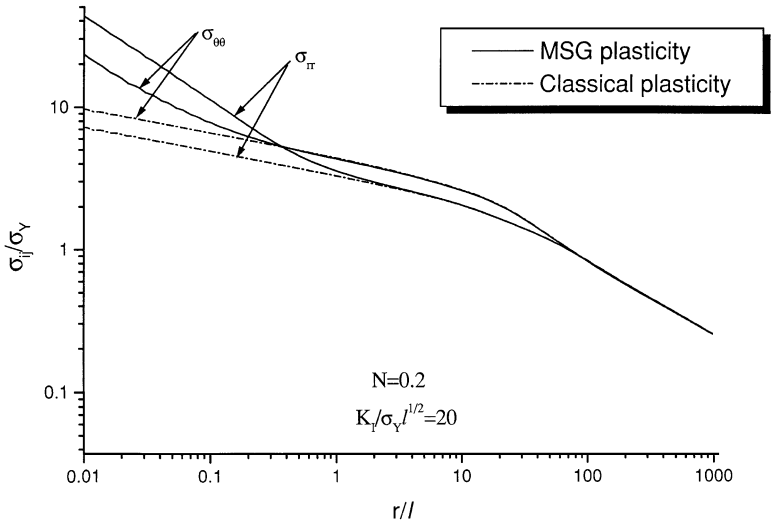

Fig. 2. The distribution of normal stresses $\sigma_{\theta\theta}$ and σ_{rr} ahead of the crack tip (polar angle $\theta = 1.014^\circ$) for both MSG plasticity and classical plasticity theories. All normalization and material and loading parameters are the same as those in Fig. 1.

small, less than 1% of $\sigma_{\theta\theta}$, because the length parameter l_ε scaling the higher-order stresses is typically one to two orders of magnitude less than the internal material length l in MSG plasticity. Accordingly, the higher-order stress traction t_θ ahead of the crack tip is essentially the same as $\sigma_{\theta\theta}$ in Fig. 2.

Fig. 3 shows the normalized effective stress, σ_e/σ_Y, versus the normalized distance to the crack tip, r/l, ahead of the crack tip (polar angle $\theta = 1.014^\circ$) for four levels of applied stress intensity factor, $K_I/\sigma_Y l^{1/2} = 2$, 5, 10 and 20. The material properties are given in (26). The interception of each curve with the horizontal line $\sigma_e/\sigma_Y = 1$ separates the plastic yielding from elastic deformation. The deformation outside the plastic zone is essentially the elastic K_I field, as evidenced by the straight line with the slope of $-1/2$ for large r. At a small distance r to the crack tip, all curves approach to another set of straight lines, with the absolute value of the slope larger or equal to $1/2$. This confirms that the crack tip field in MSG plasticity is more singular than the HRR field in classical plasticity; the order of stress singularity exceeds or equals to the square-root singularity in the elastic K_I field. It is also observed from Fig. 3 that the plastic zone size increases rapidly with the applied loading. The plastic zone size for $K_I/\sigma_Y l^{1/2} = 20$ is approximately 100 times that for $K_I/\sigma_Y l^{1/2} = 2$. However, the size of the dominance zone of the crack tip field in MSG plasticity increases relatively slow with the applied loading; the size of the dominance zone for $K_I/\sigma_Y l^{1/2} = 20$ is less than twice of that for $K_I/\sigma_Y l^{1/2} = 2$.

Fig. 4 shows the effect of plastic work hardening on the effective stress distribution ahead of the crack tip (polar angle $\theta = 1.014^\circ$). The applied stress intensity factor is $K_I/\sigma_Y l^{1/2} = 10$, and the plastic work hardening exponent are $N = 0.2$, 0.33 and 0.5. One interesting observation is that, at small distance r to the crack tip, all curves approach

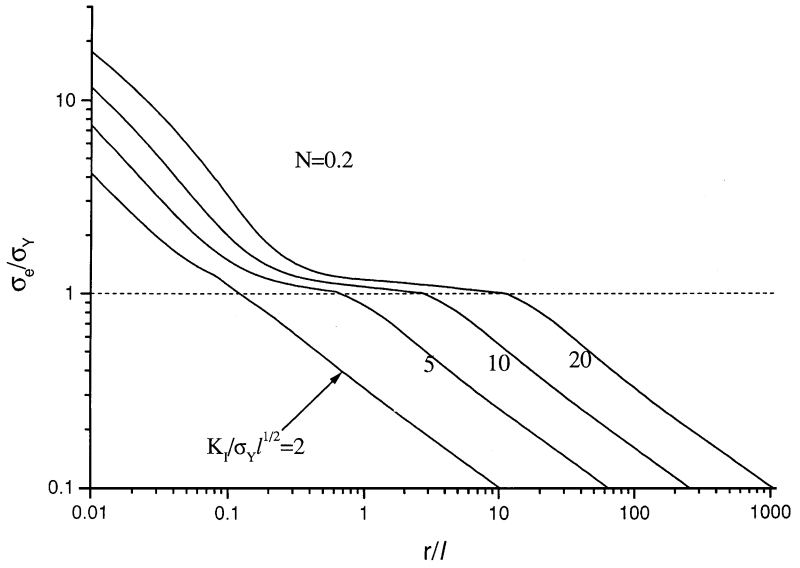

Fig. 3. The distribution of effective stress σ_e ahead of the crack tip (polar angle $\theta = 1.014^\circ$) for remotely applied elastic stress intensity factors $K_I/\sigma_Y l^{1/2} = 2$, 5, 10 and 20. All normalization and material parameters are the same as those in Fig. 1.

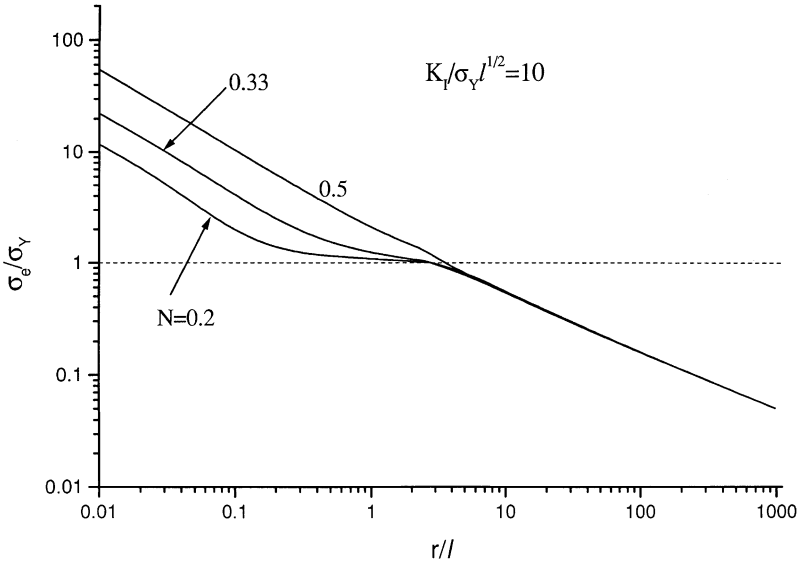

Fig. 4. The distribution of effective stress σ_e ahead of the crack tip (polar angle $\theta = 1.014^\circ$) for the remotely applied elastic stress intensity factor $K_I/\sigma_Y l^{1/2} = 10$. All normalization and material parameters are the same as those in Fig. 1, except the plastic work hardening exponent $N = 0.2$, 0.33 and 0.5.

straight lines that have the same slope. This means the crack tip singularity in MSG plasticity is essentially independent of the plastic work hardening exponent. It is, in fact, consistent with the asymptotic analysis of the crack tip field in MSG plasticity (Shi et al., 2000a). Shi et al. (2000a) showed that, near a crack tip in MSG plasticity, the strain gradient term $l\eta$ is more singular than the strain term, $\sigma_{\text{ref}}^2 f^2(\varepsilon)$, in the expression of flow stress in (16). Therefore, the strain gradient term dominates such that the crack tip field is essentially independent of the uniaxial strain–stress relation $\sigma_{\text{ref}} f(\varepsilon)$ and therefore does not depend on the plastic work hardening exponent N. The numerical results in the present study confirm this prediction. In terms of dislocation terminologies, this means that the density of geometrically necessary dislocations is much higher than that of statistically stored dislocations near a crack tip, and therefore dominates the flow stress in (16) from the Taylor model.

The above observations, in conjunction with the SSV model (Suo et al., 1993; Beltz et al., 1996), provide the following multiscale view of cleavage fracture in ductile materials: (i) At the scale as small as the dislocation spacing, the SSV model governs the crack tip behavior, i.e., there exists a core free of dislocations around the crack tip. (ii) At a larger scale that is at least one order of magnitude larger than dislocation spacing and is comparable to the internal material length l, geometrically necessary dislocations begin to dominate, and MSG plasticity governs the crack tip behavior. (iii) At a distance much larger than the internal material length l, MSG plasticity degenerates to classical plasticity, and statistically stored dislocations play a dominating role in the plastic work hardening of materials. This multiscale view of fracture provides a reasonable picture for cleavage fracture in ductile materials. It should be pointed out, however, that MSG plasticity does not degenerate to classical elasticity at small length scales. Accordingly, the crack tip field in MSG plasticity is not applicable at a distance comparable to dislocation spacing. This is evident from Fig. 2, in which stresses σ_{rr} and $\sigma_{\theta\theta}$ are different ahead of the crack tip, while their counterparts in the dislocation-free core are the same as in the classical K-field.

4. Summary

We have used the deformation theory of mechanism-based strain gradient (MSG) plasticity to investigate the stress level around a crack tip. The numerical results have shown that the stress level in MSG plasticity is significantly higher than that predicted by classical plasticity (i.e., the HRR field). At a distance that is much larger than the dislocation spacing such that continuum plasticity is expected to be applicable, the effective stress predicted by MSG plasticity is more than twice of that in classical plasticity. MSG plasticity also predicts that the crack tip stress singularity is not only larger than that in the HRR field, but also exceeds or equals to the square-root singularity. Moreover, the crack tip stress singularity is independent of the plastic work hardening exponent because geometrically necessary dislocations play a more dominating role than statistically stored dislocations near the crack tip.

The significant increase in the stress level near the crack tip has been attributed to the strain gradient effects on the mesoscale, or to geometrically necessary dislocations

on the microscale. The increase in the near-tip stress level provides an explanation to the experimental observation of cleavage fracture in ductile materials (Elssner et al., 1994). The classical plasticity theories fail to predict the stresses needed for cleavage fracture, while the significant stress increase in MSG plasticity seems to be capable of bridging the gap between the macroscopic cracking and atomistic fracture.

Acknowledgements

Y.H. acknowledges the support from US NSF (grant CMS-9896285) and NSF of China. Z.Z. and K.C.H. acknowledge the support from NSF of China.

References

Acharya, A., Bassani, J.L., 2000. Lattice incompatibility and a gradient theory of crystal plasticity. J. Mech. Phys. Solids 48, 1565–1595.

Arsenlis, A., Parks, D.M., 1999. Crystallographic aspects of geometrically-necessary and statistically-stored dislocation density. Acta Mater. 47, 1597–1611.

Ashby, M.F., 1970. The deformation of plastically non-homogeneous alloys. Philos. Mag. 21, 399–424.

Atkinson, M., 1995. Further analysis of the size effect in indentation hardness tests of some metals. J. Mater. Res. 10, 2908–2915.

Begley, M.R., Hutchinson, J.W., 1998. The mechanics of size-dependent indentation. J. Mech. Phys. Solids 46, 2049–2068.

Beltz, G.E., Rice, J.R., Shih, C.F., Xia, L., 1996. A self-consistent method for cleavage in the presence of plastic flow. Acta Mater. 44, 3943–3954.

Camacho, G.T., Ortiz, M., 1996. Computational modeling of impact damage in brittle materials. Int. J. Solids Struct. 33, 2899–2938.

Chen, J.Y., Huang, Y., Hwang, K.C., 1998. Mode I and mode II plane-stress near-tip fields for cracks in materials with strain gradient effects. Key Engng. Mater. 145, 19–28.

Chen, J.Y., Wei, Y., Huang, Y., Hutchinson, J.W., Hwang, K.C., 1999. The crack tip fields in strain gradient plasticity: the asymptotic and numerical analyses. Engng. Fract. Mech. 64, 625–648.

De Guzman, M.S., Neubauer, G., Flinn, P., Nix, W.D., 1993. The role of indentation depth on the measured hardness of materials. Mater. Res. Symp. Proc. 308, 613–618.

Elssner, G., Korn, D., Ruehle, M., 1994. The influence of interface impurities on fracture energy of UHV diffusion bonded metal-ceramic bicrystals. Scripta Metall. Mater. 31, 1037–1042.

Fleck, N.A., Hutchinson, J.W., 1993. A phenomenological theory for strain gradient effects in plasticity. J. Mech. Phys. Solids 41, 1825–1857.

Fleck, N.A., Hutchinson, J.W., 1997. Strain gradient plasticity. In: Hutchinson, J.W., Wu, T.Y. (Eds.), Advances in Applied Mechanics. Vol. 33. Academic Press, New York, pp. 295–361.

Fleck, N.A., Muller, G.M., Ashby, M.F., Hutchinson, J.W., 1994. Strain gradient plasticity: theory and experiments. Acta Metall. Mater. 42, 475–487.

Gao, H., Huang, Y., Nix, W.D., 1999a. Modeling plasticity at the micrometer scale. Naturwissenschaftler 86, 507–515.

Gao, H., Huang, Y., Nix, W.D., Hutchinson, J.W., 1999b. Mechanism-based strain gradient plasticity — I. Theory. J. Mech. Phys. Solids 47, 1239–1263.

Gurtin, M.E., 2000. On the plasticity of single crystals: free energy, microforces, plastic-strain gradients. J. Mech. Phys. Solids 48, 989–1036.

Huang, Y., Chen, J.Y., Guo, T.F., Zhang, L., Hwang, K.C., 1999a. Analytic and numerical studies on mode I and mode II fracture in elastic-plastic materials with strain gradient effects. Int. J. Fract. 100, 1–27.

Huang, Y., Gao, H., Hwang, K.C., 1999b. Strain-gradient plasticity at the micron scale. In: Ellyin, F., Provan, J.W. (Eds.), Progress in Mechanical Behavior of Materials, Vol. III, pp. 1051–1056.

Huang, Y., Gao, H., Nix, W.D., Hutchinson, J.W., 2000a. Mechanism-based strain gradient plasticity — II. analysis. J. Mech. Phys. Solids 48, 99–128.

Huang, Y., Xue, Z., Gao, H., Nix, W.D., Xia, Z.C., 2000b. A study of micro-indentation hardness tests by mechanism-based strain gradient plasticity. J. Mater. Res. 15, 1786–1796.

Huang, Y., Zhang, L., Guo, T.F., Hwang, K.C., 1995. Near-tip fields for cracks in materials with strain-gradient effects. In: Willis, J.R. (Ed.), Proceedings of IUTAM Symposium on Nonlinear Analysis of Fracture. Kluwer Academic Publishers, Cambridge, England, pp. 231–242.

Huang, Y., Zhang, L., Guo, T.F., Hwang, K.C., 1997a. Fracture of materials with strain gradient effects. In: Karihaloo, B.L., Mai, Y.W., Ripley, M.I., Ritchie, R.O. (Eds.), Advances in Fracture Research. Pergamon Press, Amsterdam, pp. 2275–2286.

Huang, Y., Zhang, L., Guo, T.F., Hwang, K.C., 1997b. Mixed mode near-tip fields for cracks in materials with strain-gradient effects. J. Mech. Phys. Solids 45, 439–465.

Hutchinson, J.W., 1997. Linking scales in mechanics. In: Karihaloo, B.L., Mai, Y.W., Ripley, M.I., Ritchie, R.O. (Eds.), Advances in Fracture Research. Pergamon Press, Amsterdam, pp. 1–14.

Hutchinson, J.W., 1968. Singular behavior at the end of a tensile crack in a hardening material. J. Mech. Phys. Solids 16, 13–31.

Lloyd, D.J., 1994. Particle reinforced aluminum and magnesium matrix composites. Int. Mater. Rev. 39, 1–23.

Ma, Q., Clarke, D.R., 1995. Size dependent hardness of silver single crystals. J. Mater. Res. 10, 853–863.

McElhaney, K.W., Vlassak, J.J., Nix, W.D., 1998. Determination of indenter tip geometry and indentation contact area for depth-sensing indentation experiments. J. Mater. Res. 13, 1300–1306.

Nan, C.-W., Clarke, D.R., 1996. The influence of particle size and particle fracture on the elastic/plastic deformation of metal matrix composites. Acta Mater. 44, 3801–3811.

Needleman, A., 1987. A continuum model for void nucleation by inclusion debonding. J. Appl. Mech. 54, 525–531.

Nix, W.D., 1989. Mechanical properties of thin films. Met. Trans. 20A, 2217–2245.

Nix, W.D., 1997. Elastic and plastic properties of thin films on substrates: nanoindentation techniques. Mater. Sci. Engr. A234–236, 37–44.

Nix, W.D., Gibeling, J.C., 1985. Mechanism of time-dependent flow and fracture of metals. Metals/Mater. Technol. Ser. 8313-004. ASM, Metals Park, OH.

Poole, W.J., Ashby, M.F., Fleck, N.A., 1996. Micro-hardness of annealed and work-hardened copper polycrystals. Scripta Metall. Mater. 34, 559–564.

Rice, J.R., Rosengren, G.F., 1968. Plane strain deformation near a crack tip in a power law hardening material. J. Mech. Phys. Solids 16, 1–12.

Shi, M.X., Huang, Y., Gao, H., Hwang, K.C., 2000a. Non-existence of separable crack tip field in mechanism-based strain gradient plasticity. Int. J. Solids Struct. 37, 5995–6010.

Shi, M.X., Huang, Y., Hwang, K.C., 2000b. Fracture in the higher-order elastic continuum. J. Mech. Phys. Solids 48, 2513–2538.

Shu, J.Y., Fleck, N.A., 1998. The prediction of a size effect in micro indentation. Int. J. Solids Struct. 35, 1363–1383.

Shu, J.Y., Fleck, N.A., 1999. Strain gradient crystal plasticity: size-dependent deformation of bicrystals. J. Mech. Phys. Solids 47, 292–324.

Stelmashenko, N.A., Walls, M.G., Brown, L.M., Milman, Y.V., 1993. Microindentation on W and Mo oriented single crystals: an STM study. Acta Metall. Mater. 41, 2855–2865.

Stolken, J.S., Evans, A.G., 1998. A microbend test method for measuring the plasticity length scale. Acta Mater. 46, 5109–5115.

Suo, Z., Shih, C.F., Varias, A.G., 1993. A theory for cleavage cracking in the presence of plastic flow. Acta Metall. Mater. 41, 1551–1557.

Tvergaard, V., Hutchinson, J.W., 1992. The relation between crack growth resistance and fracture process parameters in elastic–plastic solids. J. Mech. Phys. Solids 40, 1377–1397.

Tvergaard, V., Hutchinson, J.W., 1993. The influence of plasticity on mixed mode interface toughness. J. Mech. Phys. Solids 41, 1119–1135.

Wei, Y., Hutchinson, J.W., 1997. Steady-state crack growth and work of fracture for solids characterized by strain gradient plasticity. J. Mech. Phys. Solids 45, 1253–1273.

Wei, Y., Hutchinson, J.W., 1999. Models of interface separation accompanied by plastic dissipation at multiple scales. Int. J. Fract. 95, 1–17.

Xia, Z.C., Hutchinson, J.W., 1996. Crack tip fields in strain gradient plasticity. J. Mech. Phys. Solids 44, 1621–1648.

Xu, X.-P., Needleman, A., 1994. Numerical simulations of fast crack growth in brittle solids. J. Mech. Phys. Solids 42, 1397–1434.